

Properties of neutron stars and strangeness-mixed stars from a pion mean-field approach

Nam-Yong Ghim,^{1,*} Hyun-Chul Kim,^{1,2,†} Ulugbek Yakshiev,^{1,3,4,‡} and Ghil-Seok Yang^{5,§}

¹*Department of Physics, Inha University, Incheon 22212, Republic of Korea*

²*School of Physics, Korea Institute for Advanced Study (KIAS), Seoul 02455, Republic of Korea*

³*Department of Physics, New Uzbekistan University, Tashkent 100007, Uzbekistan*

⁴*Theoretical Physics Department, National University of Uzbekistan, Tashkent 100174, Uzbekistan*

⁵*Department of General Education for Human Creativity, Hoseo University, Asan 31499, Republic of Korea*

We investigate the properties of the static neutron stars and strangeness-mixed stars, based on the equations of state derived from a pion mean-field approach. Using the empirical data on the pion-nucleus scattering and bulk properties of nuclear matter, we have already fixed all the parameters in a previous work, where the nucleons and hyperons were shown to be modified in various nuclear medium. In the current work, we first examine the energy and pressure inside a neutron star. We show that the central densities in various neutron stars vary within the range of $(3 - 6)\rho_0$, where ρ_0 is the normal nuclear matter density. The mass-radius relations are obtained and discussed. As the slope parameter for neutron matter increases, the radii of the neutron stars increase with their masses fixed. We also study the strangeness-mixed stars or the hyperon stars using the same sets of the parameters. As the strangeness content of strange matter increases, the binding energy per nucleon is saturated and the corresponding equation of state becomes softened. Consequently, the central densities of the strangeness-mixed stars increase. Assuming that recently observed neutron stars are the strangeness-mixed ones, we find that the central densities increase. In the case of the pure strange stars, the central densities reach almost $(5 - 6)\rho_0$.

Keywords: neutron stars, neutron matter, strange matter, pion mean-field approach

I. INTRODUCTION

Neutron stars are known to form strongly interacting cold-dense neutron matter, so that they provide a test ground for the equation of state (EoS) derived from many theories and models [1, 2]. The data on the masses and radii of the neutron stars have been compiled from astronomical observations such as low mass X-ray binaries [3–10] for decades. Demorest et al. [11] observed the binary millisecond pulsar J1614-2230 from which its mass was estimated to be $(1.97 \pm 0.04)M_\odot$. Antoniadis et al. [12] made a radio-timing observations of the PSR J0348+0432 and evaluated the mass of the neutron star as $(2.01 \pm 0.04)M_\odot$. Fonseca et al. [13] analyzed 24 binary radio pulsars for nine years and found the mass range of the neutron stars between $1.18 M_\odot$ and $1.93 M_\odot$. In a recent paper [14], the pulsar mass was estimated to be $2.08 M_\odot$ from the observations of PSR J0740+6620. Very recently, the observation of gravitational waves have further sharpened the data on the neutron stars [15–17]. The proposed Einstein Telescope in Europe [18–20] and the Cosmic Explorer in the US [21, 22], which are ten times sensitive future third-generation gravitational-wave observatories, are expected to provide more precise information on the nature of neutron stars in the future. The Neutron Star Interior Composition Explorer (NICER) experiment observed PSR J0030+0451, from which the radius and mass of the neutron star were inferred to be $R = 13.02^{+1.24}_{-1.06}$ km and $M = 1.44^{+0.15}_{-0.14} M_\odot$ [23]. On the other hand, Riley et al. [24] estimated them as $12.39^{+1.30}_{-0.98}$ km and $2.072^{+0.067}_{-0.066} M_\odot$. We anticipate that the NICER will bring more essential data [25, 26], which can further constrain the EoS for neutron star matter (see also recent reviews and references therein [27, 28]). The mass of black widow [29], which is the fastest and heaviest known galactic neutron star, was estimated to be $M = (2.35 \pm 0.17)M_\odot$. Its observation can also constrain the EoS.

In the present work, we aim at investigating the masses and radii of the neutron stars, based on the pion mean-field approach or the chiral quark-soliton model (χ QSM) [30–32]. The idea was motivated by Witten’s seminal paper [33]: In the large N_c (the number of colors) limit the presence of N_c valence quarks creates the pion mean fields self-consistently. Since the mesonic quantum fluctuations are suppressed in the large N_c limit, a baryon emerges as a state of N_c valence quarks bound by the pion mean fields. This approach was successful in describing many properties of the low-lying baryons such as mass splittings [34–36], static properties [37–43], form factors [44–48], parton distribution

* Namyong.gim@inha.edu

† hchkim@inha.ac.kr

‡ yakshiev@inha.ac.kr

§ ghsyang@hoseo.edu

functions [49, 50], and so on. A great merit of the pion mean-field approach lies in the fact that both the light and singly heavy baryons can be explained on an equal footing. Replacing a light valence quark with a heavy quark, we find that the singly heavy baryon arises as the bound state of the $N_c - 1$ valence quarks by the pion mean fields. A heavy quark can be regarded as a static color source in the limit of the infinitely large mass of the heavy quark [51–60] (see also a recent review [61]).

The pion mean-field approach can also be extended to the investigation of nuclear matter and medium modification of baryons in it. While one can introduce the quark chemical potential and examine quark matter [62, 63], it is difficult to associate quark matter with nuclear matter directly. Thus, we employ a variational approach that was successfully used in the medium modified Skyrme models [64–69]. A virtue of the variational approach is that the dynamical parameters can be fixed by considering low-energy pion-nucleus scattering and reproducing saturation and bulk properties of homogeneous nuclear matter. In fact, the general structure of the flavor SU(3) collective Hamiltonian arises from the embedding of the SU(2) soliton into SU(3) [70, 71]. Thus, the collective Hamiltonian can be constructed based on $SU(2)_T \otimes U(1)_Y$ symmetry [35, 36]. Thus, while we derive the collective Hamiltonian, we fix the dynamical parameters by reproducing the properties of nuclear matter. Recently, we studied the medium modification of the low-lying SU(3) baryons in four different cases, i.e. symmetric matter, asymmetric matter, neutron matter, and strange baryonic matter consistently, based on a pion mean-field approach [72]. We were able to explain the properties of nuclear matter such as the binding energy per nucleon, symmetric energy, pressure, and medium modifications of the low-lying SU(3) baryons and singly heavy baryons [73]. Thus, we want to examine the masses and radii of neutron stars, using the EoS developed in Refs. [72, 73]. This approach has two significant virtues: First, since we have already fixed all necessary dynamical parameters, we do not need to perform any additional fitting procedure to evaluate the masses and radii of neutron stars, which will indeed play a role of the touchstone for the EoS developed in the pion mean-field approach. Second, the medium modifications of the nucleon were consistently considered.

The current work is organized as follows: In Sec. II, we recapitulate the pion mean-field approach, focusing on the collective Hamiltonian and a medium modification of the model using the variational approach. In Sec. III, we examine the mass, energy, and pressure densities, which will be used in the Tolman-Oppenheimer-Volkoff (TOV) equation. In Sec. IV, we discuss the results for the masses and radii of the neutron stars, and then we extend the formalism to investigate the hybrid stars, employing the strange matter. In Sec. V, we draw conclusions and summarize the current work.

II. PION MEAN-FIELD APPROACH

The χ QSM is based on the low-energy QCD partition function in Euclidean space

$$\mathcal{Z}_{\text{eff}} = \int D\psi D\psi^\dagger D\pi^a \exp \left[\int \psi^\dagger (i\partial + iMU\gamma_5 + i\hat{m})\psi \right] = \int D\pi^a \exp(-S_{\text{eff}}[\pi^a]), \quad (1)$$

where ψ and ψ^\dagger denote the quark fields and π^a stand for the pseudo-Goldstone fields. $S_{\text{eff}}[\pi^a]$ is the effective chiral action defined by

$$S_{\text{eff}}[\pi^a] := -N_c \text{Tr} \log (i\partial + iMU\gamma_5 + i\hat{m}), \quad (2)$$

where M represents the dynamical quark mass. It is originally the momentum-dependent one, which was derived from the fermionic zero mode of individual instantons [74, 75]. For simplicity, we turn off the momentum dependence of M and introduce the regularization to tame the quark fields. $U\gamma_5$ denotes the chiral field expressed as

$$U\gamma_5(x) = \exp(i\pi^a(x)\lambda^a\gamma_5) = U(x)\frac{1+\gamma_5}{2} + U^\dagger(x)\frac{1-\gamma_5}{2} \quad (3)$$

with $U(x) = e^{i\pi^a(x)\lambda^a}$. \hat{m} designates the current quark mass matrix written as

$$\hat{m} = \begin{pmatrix} m_u & 0 & 0 \\ 0 & m_d & 0 \\ 0 & 0 & m_s \end{pmatrix} = m_0 \mathbf{1} + m_3 \lambda^3 + m_8 \lambda^8 \quad (4)$$

with

$$m_0 = \frac{m_u + m_d + m_s}{3}, \quad m_3 = \frac{m_u - m_d}{2}, \quad m_8 = \frac{m_u + m_d - 2m_s}{2\sqrt{3}}. \quad (5)$$

Here, λ^a represent the Gell-Mann matrices for the flavor SU(3) group and m_u , m_d , and m_s denote the current up, down, and strange quark masses, respectively. The effective chiral action contains all orders of the effective chiral Lagrangians with the low-energy constants, which can be derived from the gradient expansion [30, 76].

The classical nucleon mass or the chiral soliton mass can be obtained by solving the nucleon correlation function. By solving the correlation function, we mean that the N_c valence quarks are positioned in the lowest level bound by the pion mean fields produced by the presence of the N_c valence quarks self-consistently. Since the mesonic quantum fluctuations are known to be suppressed in the large N_c limit [33], we can integrate over the pseudo-Goldstone boson fields in Eq. (1) around the saddle point $U_c(\mathbf{x})$. The equation of motion for the quarks with the classical pion fields can be minimized by the Hartree approximation, we obtain the pion mean fields with hedgehog symmetry

$$U_c(\mathbf{x}) = \exp(i\boldsymbol{\tau} \cdot \mathbf{n}P(r)), \quad (6)$$

where $P(r)$ is called the profile function. In the current work, we will not follow the self-consistent procedure to determine the profile functions and classical soliton mass. Instead, we will maximally use the $SU(2)_T \otimes U(1)_Y$ symmetry that arises from the embedding of the SU(2) chiral soliton into SU(3)

$$U(\mathbf{x}) = \begin{pmatrix} U_c(\mathbf{x}) & 0 \\ 0 & 1 \end{pmatrix}. \quad (7)$$

The dynamical parameters will be determined by using the experimental and empirical data. This method is often called “*a model-independent*” approach for the chiral soliton, which has a virtue when it is extended to the investigation of bulk properties of nuclear matter and baryon properties in it.

Since the classical soliton does not carry quantum numbers of baryons, we need to quantize it. As mentioned already, the quantum fluctuations of the pion fields are suppressed by the large N_c approximation. On the other hand, the fluctuation of the pion field to the zero-mode directions, which are always related to translational and rotational symmetries, must be considered. Rotational zero modes determine the quantum numbers of baryons. For details, we refer to Refs. [31, 32]. Having performed the zero-mode quantization, we derive the collective Hamiltonian [34–36]

$$H = M_{\text{cl}} + H_{\text{rot}} + H_{\text{sb}} + H_{\text{em}}, \quad (8)$$

where M_{cl} denotes the mass of the classical nucleon. H_{rot} stands for the rotational $1/N_c$ corrections arising from the zero-mode quantization

$$H_{\text{rot}} = \frac{1}{2I_1} \sum_{i=1}^3 \hat{J}_i^2 + \frac{1}{2I_2} \sum_{p=4}^7 \hat{J}_p^2, \quad (9)$$

where the $I_{1,2}$ are the moments of inertia and \hat{J}_a ($a = 1, \dots, 8$) are the generators of the the SU(3) group, which are directly related to the right angular velocities Ω_a . The eighth component of J_a is constrained to be

$$J_8 = -\frac{N_c}{2\sqrt{3}}B = -\frac{\sqrt{3}}{2}, \quad (10)$$

where B is the baryon number. J_8 is related to the right hypercharge $Y_R = -Y' = (2/\sqrt{3})J_8$. While in the Skyrme model J_8 is constrained by the Wess-Zumino term, the presence of the N_c valence quarks constrained it within the current approach. The constraint (10) has significant physical implications: It selects the lowest allowed representations. If the baryon multiplet with $Y = 1$ consists of $2J + 1$ multiplet, the spin of the multiplet is set to be J . Thus, the baryon octet and decuplet are selected. In the representation $\mathcal{R} = (p, q)$, the eigenvalues of the Hamiltonian H_{rot} in Eq. (9) are given as

$$E_{(p,q),J} = \frac{1}{2} \left(\frac{1}{I_1} - \frac{1}{I_2} \right) J(J+1) - \frac{3}{8I_2} + \frac{1}{6I_2} (p^2 + q^2 + 3(p+q) + pq). \quad (11)$$

The third term in Eq. (8) stands for both the isospin and SU(3) flavor symmetry breaking part

$$\begin{aligned} H_{\text{sb}} = & (m_d - m_u) \left(\frac{\sqrt{3}}{2} \alpha D_{38}^{(8)}(\mathcal{A}) + \beta \hat{T}_3 + \frac{1}{2} \gamma \sum_{i=1}^3 D_{3i}^{(8)}(\mathcal{A}) \hat{J}_i \right) \\ & + (m_s - \bar{m}) \left(\alpha D_{88}^{(8)}(\mathcal{A}) + \beta \hat{Y} + \frac{1}{\sqrt{3}} \gamma \sum_{i=1}^3 D_{8i}^{(8)}(\mathcal{A}) \hat{J}_i \right), \end{aligned} \quad (12)$$

where the α , β , γ expressed in terms of the moments of inertia

$$\alpha = -\left(\frac{2}{3}\frac{\Sigma_{\pi N}}{m_u + m_d} - \frac{K_2}{I_2}\right), \quad \beta = -\frac{K_2}{I_2}, \quad \gamma = 2\left(\frac{K_1}{I_1} - \frac{K_2}{I_2}\right). \quad (13)$$

Here $K_{1,2}$ represents the anomalous moments of inertia of the rotating soliton. The \bar{m} is the average value of the up and down current quark masses, i.e. $\bar{m} = (m_u + m_d)/2$. The $D_{ab}^{(\mathcal{R})}$ are the SU(3) Wigner D functions in a given representation \mathcal{R} . The explicit form of the electromagnetic (EM) self-energy term H_{em} is given in Ref. [35]. However, the effects of the EM self-energies are negligibly small for medium modification [65, 66], we ignore them in the current work.

The dynamical parameters α , β , and γ can be evaluated within the self-consistent SU(3) χ QSM. However, we will adopt the model-independent approach, as previously mentioned. So, we will fix all dynamical parameters by using the experimental data rather than by computing within the model [36, 77]. Furthermore, we employ the variational method to modify the collective Hamiltonian (8) in nuclear medium. We briefly recapitulate the general formalism for the medium modification of H . For details, we refer to Refs. [72, 73].

In Refs. [72, 73], three different types of nuclear environments were considered, i.e. the isospin symmetric, isospin asymmetric, and strangeness-mixed nuclear matters. Thus, we introduce three corresponding parameters as follows:

$$\lambda = \frac{n}{n_0}, \quad \delta = \frac{N - Z}{A}, \quad \delta_s = \frac{N_s}{A}, \quad (14)$$

where λ is the density of nuclear matter normalized by the normal nuclear matter density $\rho_0 \simeq 2.7 \times 10^{14} \text{ g/cm}^3$ ($n_0 = 0.16$ nucleons per fm^3). The isospin asymmetry in nuclear matter is controlled by δ , which is related to the number of neutrons N , of protons Z , and of baryons A . The last variational parameter δ_s is responsible for the strangeness mixing ratio that is proportional to the number of baryons N_s with strangeness $s = |S|$. Using these three parameters, we can define the binding energy per baryon as

$$\begin{aligned} \varepsilon(\lambda, \delta, \delta_1, \delta_2, \delta_3) &= \Delta M_N(\lambda, \delta, \delta_1, \delta_2, \delta_3) \left(1 - \sum_{s=1}^3 \delta_s\right) + \frac{1}{2} \delta \Delta M_{np}(\lambda, \delta, \delta_1, \delta_2, \delta_3) \\ &+ \sum_{s=1}^3 \delta_s \Delta M_s(\lambda, \delta, \delta_1, \delta_2, \delta_3). \end{aligned} \quad (15)$$

See Ref. [72] for details. As a result, we have the following density-dependent classical nucleon mass M_{cl}^* , the moments of inertia $I_{1,2}^*$, the in-medium modified isospin symmetry breaking¹ E_{iso}^* and the SU(3) symmetry breaking E_{str}^* terms:

$$M_{\text{cl}}^* = M_{\text{cl}} f_{\text{cl}}(\lambda, \delta, \delta_1, \delta_2, \delta_3), \quad (16)$$

$$I_1^* = I_1 f_1(\lambda, \delta, \delta_1, \delta_2, \delta_3), \quad (17)$$

$$I_2^* = I_2 f_2(\lambda, \delta, \delta_1, \delta_2, \delta_3), \quad (18)$$

$$E_{\text{iso}}^* = (m_d - m_u) \frac{K_{1,2}}{I_{1,2}^*} f_0(\lambda, \delta, \delta_1, \delta_2, \delta_3), \quad (19)$$

$$E_{\text{str}}^* = (m_s - \bar{m}) \frac{K_{1,2}}{I_{1,2}^*} f_s(\lambda, \delta, \delta_1, \delta_2, \delta_3), \quad (20)$$

where f_{cl} , $f_{0,1,2}$, and f_s are given as the functions of the baryon environment densities and other medium parameters.

¹ Here, the strong part of the in-medium modified effects on isospin symmetry breaking are presented.

These functions are explicitly written as

$$f_{\text{cl}}(\lambda) = (1 + C_{\text{cl}}\lambda), \quad (21)$$

$$f_{1,2}(\lambda) = (1 + C_{1,2}\lambda), \quad (22)$$

$$f_0(\lambda, \delta) = 1 + \frac{C_{\text{num}}\lambda\delta}{1 + C_{\text{den}}\lambda}, \quad (23)$$

$$f_s(\lambda, \delta_s) = 1 + g_s(\lambda)\delta_s \quad (24)$$

$$g_s(\lambda) = sg(\lambda), \quad (25)$$

$$g(\lambda) = \left(6\frac{K_2}{I_2} + \frac{K_1}{I_1}\right)^{-1} \times \frac{5(M_{\text{cl}} - M_{\text{cl}}^* + E_{(1,1)1/2} - E_{(1,1)1/2}^*)}{3(m_s - \hat{m})}, \quad (26)$$

where the C_{cl} , C_1 , C_2 , C_{num} , C_{den} , which are fixed by reproducing the bulk properties of nuclear matter [72]

$$C_{\text{cl}} = -0.0561, \quad C_1 = 0.6434, \quad C_2 = -0.1218, \quad C_{\text{num}} = 65.60, \quad C_{\text{den}} = 0.60. \quad (27)$$

We find that the present medium-modified EoS describes very well bulk properties of nuclear matter and symmetry energies up to density $\sim 3\rho_0$. Even at higher densities, the results are in reasonable agreement with empirical data. We want to examine the EoS developed in Ref. [72] by computing the mass-radius relation of neutron stars in the current work. For simplicity, we also introduce the common strangeness mixing parameter χ as

$$\sum_s s\delta_s = \chi, \quad (28)$$

where s is the strangeness of the hyperon. Then the binding energy per baryon is given as a function of three parameters $\varepsilon = \varepsilon(\lambda, \delta, \chi)$.

The nuclear symmetry energy is defined as the second derivative of the binding energy with respect to δ

$$\varepsilon_{\text{sym}}(\lambda) = \frac{1}{2!} \left. \frac{\partial^2 \varepsilon(\lambda, \delta, 0, 0, 0)}{\partial \delta^2} \right|_{\delta=0}. \quad (29)$$

ε_{sym} can be expanded in the vicinity of the saturation point $\lambda = 1$

$$\varepsilon_{\text{sym}}(\lambda) = a_{\text{sym}} + \frac{L_{\text{sym}}}{3}(\lambda - 1) + K_{\text{sym}} \frac{(\lambda - 1)^2}{18} + \dots, \quad (30)$$

where a_{sym} denotes the nuclear symmetry energy at saturation point, L_{sym} stands for that of its slope parameter L_{sym} , and K_{sym} represents the asymmetric part of the incompressibility. They are expressed as

$$a_{\text{sym}} = -\frac{9}{20} \frac{C_{\text{num}}(b - 7r/18)}{(1 + C_{\text{den}})}, \quad (31)$$

$$L_{\text{sym}} = -\frac{27}{20} \frac{C_{\text{num}}(b - 7r/18)}{(1 + C_{\text{den}})^2}, \quad (32)$$

$$K_{\text{sym}} = \frac{81C_{\text{den}}C_{\text{num}}(b - 7r/18)}{10(1 + C_{\text{den}})^3}, \quad (33)$$

where $b = (m_{\text{d}} - m_{\text{u}})\beta$ and $r = (m_{\text{d}} - m_{\text{u}})\gamma$. The empirical values of a_{sym} and L_{sym} are known to be $a_{\text{sym}} = (31.7 \pm 3.2)$ MeV and $L_{\text{sym}} = (58.7 \pm 28.1)$ MeV, respectively [2]. In the current work, we take four different sets of parameters for a_{sym} and L_{sym} as shown in Table I.

The density dependence of the symmetry energy is constrained by the experimental data on heavy-ion collision [78–81]. In the previous work [72], we showed that the results for $\varepsilon(\lambda)$ are in good agreement with the APR predictions [82] and IAS constraints [83]. The values of a_{sym} and L_{sym} are also very similar to those in various theoretical works [1, 10, 84, 85]. As will be shown later, the results for the masses and radii of the neutron stars are not sensitive to changes of the symmetry energy, whereas its slope parameter has certain effects on them. In Ref. [72], we also discussed as to how the parameters, K_{sym} and related incompressibilities, were determined in detail. The results for both the energy and pressure indicate that the slope parameter of the symmetric energy will influence the mass-radius relations of the neutron stars.

Table I. Four different sets of the parameters for the symmetry energy and slope parameter at the normal nuclear matter density ρ_0 .

	a_{sym} [MeV]	L_{sym} [MeV]	C_{num}	C_{den}
Set I	30	50	69.20	0.80
Set II	32	50	78.72	0.92
Set III	30	60	57.66	0.50
Set IV	32	60	65.60	0.60

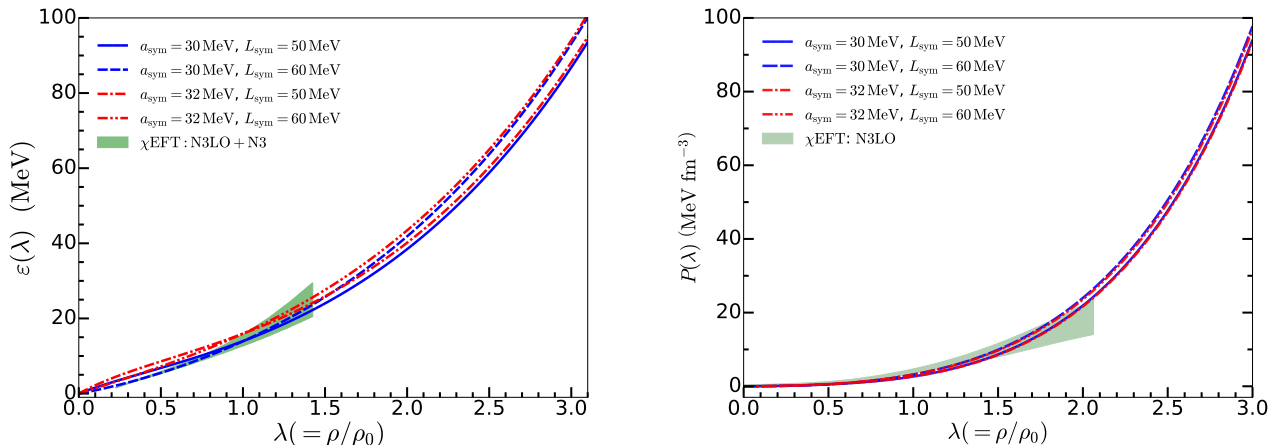


Figure 1. The energy and pressure as functions of λ . The parameters in the legend correspond to those given in Table I. The green area represents the results from Ref. [86].

The left panel of Fig. 1 depicts the binding energy per nucleon for neutron matter as a function of λ , of which the expression is given by Eq. (15) with $\delta = 1$ and $\delta_s = 0$. The current results are in good agreement with those obtained in chiral effective theory [86] with the three-loop order corrections and three-body interaction considered. We find one interesting feature of the slope parameter L_{sym} . When λ is small, the symmetry energy governs the behavior of the energy per nucleon. As λ increases, the slope parameter takes charge of it. The right panel of Fig. 1 draws the pressure as a function λ . We also compare the results with those from Ref. [86]. As observed in the right panel of Fig. 1, a larger value of the slope parameter, i.e., $L_{\text{sym}} = 32$ MeV enhances the pressure. On the other hand, the change of the symmetry energy shows only a tiny effect on the pressure.

III. ENERGY DENSITIES AND PRESSURES FOR NEUTRON STARS

To study the mass-radius relation of the neutron stars, we consider static and spherically symmetric non-rotating neutron stars, which satisfies the Tolman-Oppenheimer-Volkoff (TOV) equation. The mass function of the neutron star $M(r)$ is given as a function of radius r

$$\mathcal{M}(r) = 4\pi \int_0^r dr r^2 \mathcal{E}(r), \quad (34)$$

where $\mathcal{E}(r)$ stands for the energy density as a function of r . Then the total mass of the neutron star with radius R is defined by

$$M = \mathcal{M}(R). \quad (35)$$

The pressure $P(r)$ is determined by solving the TOV equation

$$\frac{dP(r)}{dr} = \frac{\mathcal{E}(r)\mathcal{M}(r)}{r^2} \left(1 - \frac{2\mathcal{M}(r)}{r}\right)^{-1} \left(1 + \frac{P(r)}{\mathcal{E}(r)}\right) \left(1 + \frac{4\pi r^2 P(r)}{\mathcal{M}(r)}\right) \quad (36)$$

in natural units $c = G = 1$. The boundary conditions for the mass and energy densities at the center of the neutron star are given as

$$\mathcal{M}(0) = 0, \quad \mathcal{E}(0) = \mathcal{E}_c, \quad (37)$$

where the \mathcal{E}_c is the central energy density of the neutron star. The stability condition requires the local pressure to be zero at the surface of the neutron star

$$P(R) = 0. \quad (38)$$

To obtain the profile of a neutron star, we need to know the energy dependence of the pressure

$$P = P(\mathcal{E}), \quad (39)$$

which can be derived from the following equation

$$\begin{aligned} P(\lambda, \delta, \chi) &= \rho_0 \lambda^2 \frac{\partial \mathcal{E}(\lambda, \delta, \chi)}{\partial \lambda}, \\ \mathcal{E}(\lambda) &= [\varepsilon(\lambda, \delta, \chi) + m_N] \lambda \rho_0. \end{aligned} \quad (40)$$

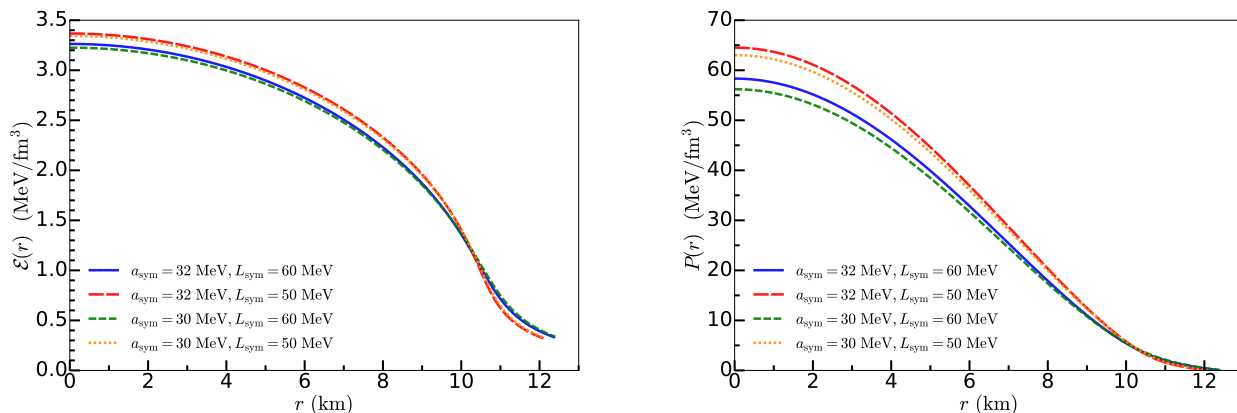


Figure 2. The energy density and pressure of the neutron star as functions of r .

The numerical result for $\mathcal{E}(r)$ is drawn in the left panel of Fig. 2 with the value of the incompressibility $K_0 = 240$ MeV. The results are rather stable as the parameters are changed. As expected, the energy density falls off monotonically, as r increases, and then it slowly vanishes at the surface of the neutron star. The right panel of Fig. 2 shows the interior pressure of the neutron star as a function of r , which is obtained by solving Eq. (36). The pressure also drops off as r increases, and vanishes at around 11-12 km, which corresponds to the radius of the neutron star. Using Eq. (35) and (38), we can derive the masses and radii of the neutron stars.

IV. RESULTS AND DISCUSSIONS

A. Neutron stars

Since all the parameters were determined in the previous work [72], we do not change any parameters for evaluating the masses and radii of the neutron stars. Using the four different sets of parameters listed in Table I, we proceed to compute the mass-radius relations of the neutron stars.

In Fig. 3, we show the masses of the neutron star in units of the solar mass as functions of dimensionless central density λ with the four different parameter sets used. While the results are not sensitive to a_{sym} , they depend on L_{sym} in lower nuclear matter density. The results indicate that the central density of the neutron stars observed in Refs. [12–14] is approximately $\lambda \approx 4$ or $\rho \approx 0.64 \text{ fm}^{-3}$. On the other hand, The central density for the neutron star from GW190814 [87] is around $\lambda \approx 6$ or $\rho \approx 0.96 \text{ fm}^{-3}$. The masses of the neutron stars are almost saturated at around $M \approx 2.5M_{\odot}$.

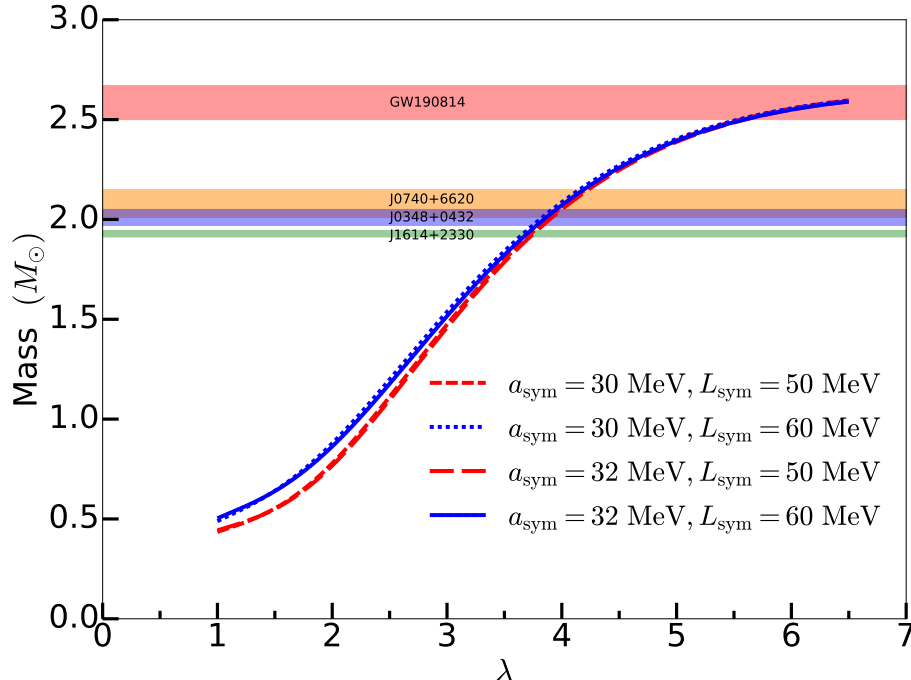


Figure 3. Masses of the neutron star are drawn as functions of the dimensionless central density $\lambda = \rho/\rho_0$ with $\rho_0 = 0.16 \text{ fm}^{-3}$ in unit of the solar mass M_\odot . The red bar corresponds to the data from Ref. [87]. The data for the orange, blue, and green bars are taken from Refs. [12–14].

It is interesting to compare the current results with those from other approaches. In Ref. [82], Akmal et al. constructed the EoS by using the Argonne nucleon-nucleon potential (A18), Urbana three-nucleon interactions, the boost interaction, and the estimated maximum masses of $M = 2.2M_\odot$ at $\lambda \approx 6$. Baym et al. [28] also obtained the maximum masses of $M = 2.2M_\odot$ saturated at around $\lambda \approx 6$. On the other hand, Brandes et al. [88] incorporated the data on the newly observed neutron called the black-widow (PSR J0952-0607) [29], and estimated $\lambda \approx 4$ for $M = 2.1M_\odot$. Vijayan et al. [89] reported very interesting results. Using two different EoS and considering the medium modification of the pion mass, they found that the central density reaches $\lambda \approx 6$ for $M = (1.7 - 2.3)M_\odot$. Since the current framework has naturally taken into account the medium modifications of hadrons, the present results are in good agreement with those from Ref. [29].

Figure 4 depicts the mass-radius relations for the neutron stars. As already discussed above, the mass-radius relations are not sensitive to a_{sym} , the radius tends to increase as the slope parameter L_{sym} increases, in particular, when the neutron matter density is low. As the density increases, the dependence of the mass-radius relations on L_{sym} becomes smaller. Figure 4 also indicates that the central densities in PSR J0740+6620, PSR J0348+0432, and PSR J1614+2330 [12–14] are estimated to be around $3.5\rho_0$. The current calculation estimates the central density of the neutron star from GW190814 [87] to be around $6.5\rho_0$. When $L_{\text{sym}} = 50 \text{ MeV}$ is used, the radii of the neutron stars are approximately 12 km except for that from the neutron star corresponding to GW190814, of which the radius is around 11 km. On the other hand, if we employ $L_{\text{sym}} = 60 \text{ MeV}$, the radii of the neutron stars tend to increase, i.e. $R \approx 12.5 \text{ km}$, again except for that from GW190814, which remains almost stable as L_{sym} is changed.

The empirical values of the nuclear matter incompressibility K_0 are given in a wide range. For example, the value of K_0 was often predicted as $K_0 \approx (290 \pm 70) \text{ MeV}$ [91–96]. In Ref. [97], however, a smaller value was extracted from the data on the isoscalar giant monopole resonance in ^{208}Pb , based on relativistic mean-field models: $K_0 = (248 \pm 8) \text{ MeV}$. In Ref. [98], $K_0 = (240 \pm 20) \text{ MeV}$ was extracted from a reanalysis of the data on the energies of the giant monopole resonances in even-even $^{112-124}\text{Sn}$ and $^{106,100-116}\text{Cd}$ and earlier data on $58 \leq A \leq 208$ nuclei. A similar value was also estimated in Ref. [99]. Thus, while we choose $K_0 = 240 \text{ MeV}$, it is of great interest to examine the dependence of the mass-radius relations of the neutron stars on K_0 . In Fig. 5, we demonstrate the mass-radius relations of the neutron stars, varying the incompressibility of nuclear matter K_0 from 210 MeV to 260 MeV. We take the values of $a_{\text{sym}} = 32 \text{ MeV}$ and $L_{\text{sym}} = 60 \text{ MeV}$. The tendency of the mass-radius relations is obvious in general. If we increase K_0 from 220 MeV to 260 MeV, the mass-radius relations remain as almost the same shape but are shifted to the right.

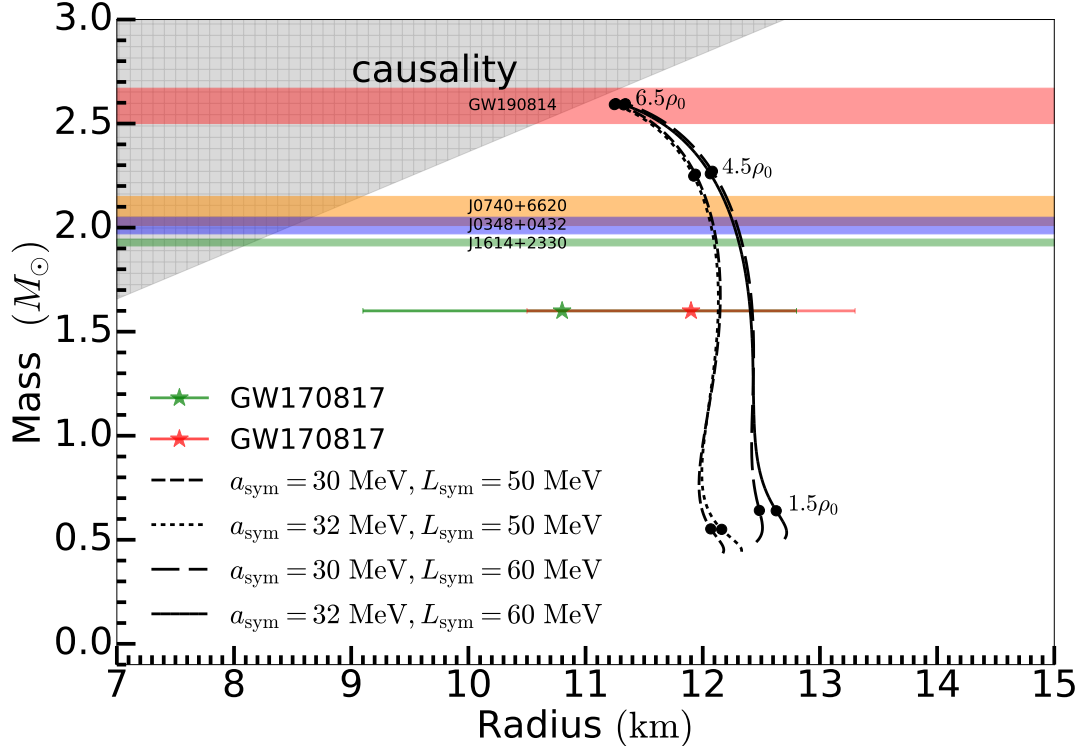


Figure 4. Mass-radius relations of neutron stars. The black curves represent the results with the four different sets of parameters given in Table I. The value of the incompressibility is chosen as $K_0 = 240$ MeV. The red and green lines with stars are taken from the LIGO experimental data [90]. The red bar corresponds to the data from Ref. [87]. The data for the orange, blue, and green bars are taken from Ref. [12–14].

So, the radii of the neutron stars get larger as K_0 increases.

In Table II, we list the results for the central densities and the radii, which correspond to two different values of the neutron star masses, i.e. $M = 1.4M_\odot$ and $M = 2.0M_\odot$. We take different values of K_0 with two different sets of parameters for neutron matter. The results show that as K_0 increases, the central density decreases, so the radius of the neutron star enlarges.

B. Strangeness-mixed stars

A virtue of the current approach is that we can easily incorporate the hyperons into nuclear matter. As shown in Eq. (14), the parameter δ_s controls the proportionality of the hyperons with strangeness $s = |S|$. Thus, the energy density can depend on δ_s as in Eq. (15). Once we construct the EoS for baryonic matter with strangeness, we can evaluate the mass-radius relations of hyperon stars. Before we compute them, we will recapitulate how baryonic matter can be formulated within the present approach. Note that we will not introduce any new parameters but introduce the hyperons with strangeness $s = |S|$.

We first expand the binding energy per baryon given in Eq.(15) with respect to isospin-asymmetry parameter δ and strangeness-mixing parameters δ_s

$$\begin{aligned} \varepsilon(\lambda, \delta, \delta_1, \dots) = & \varepsilon_V(\lambda) + \varepsilon_{\text{sym}}(\lambda) \delta^2 + \sum_{s=1}^3 \left. \frac{\partial \varepsilon(\lambda, \delta, \delta_1, \dots)}{\partial \delta_s} \right|_{\delta=\delta_1=\dots=0} \delta_s \\ & + \frac{1}{2} \sum_{s,p=1}^3 \left. \frac{\partial^2 \varepsilon(\lambda, \delta, \delta_1, \dots)}{\partial \delta_s \partial \delta_p} \right|_{\delta=\delta_1=\dots=0} \delta_s \delta_p + \dots, \end{aligned} \quad (41)$$

where the first and second terms denote the volume and symmetry energies for ordinary nuclear matter. It is obvious

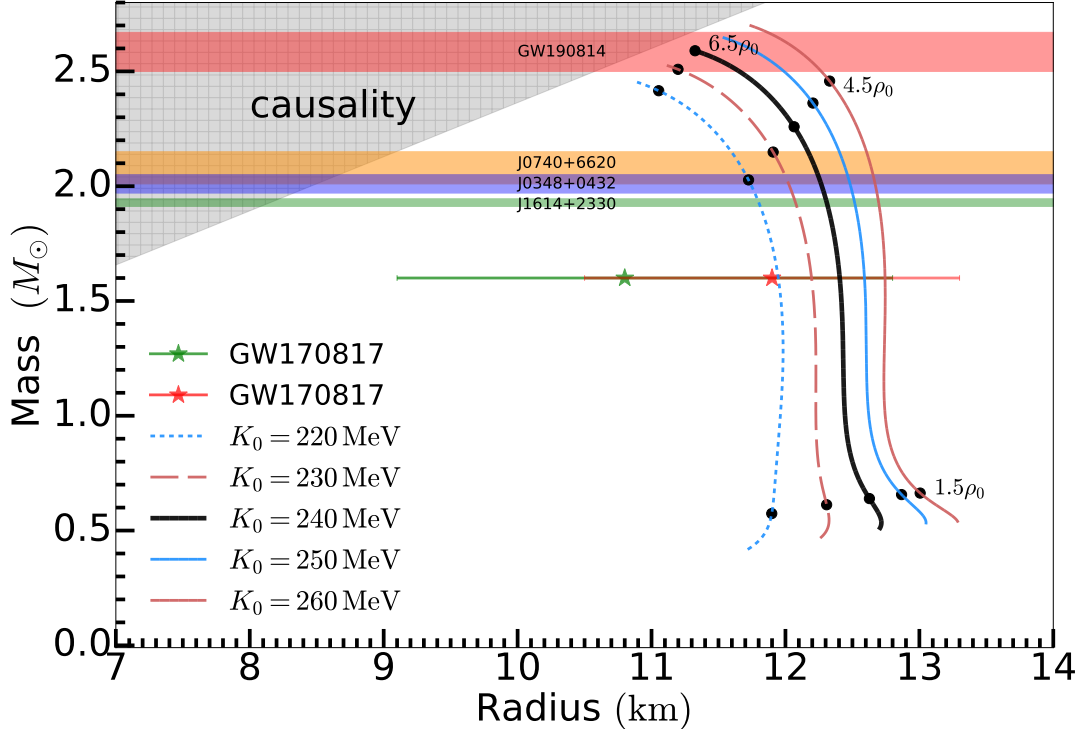


Figure 5. Dependence of the neutron star mass-radius relation on the incompressibility, K_0 . The values of the symmetry energy at saturation density and the corresponding slope parameter are chosen as $a_{\text{sym}} = 32$ MeV and $L_{\text{sym}} = 60$ MeV, respectively. The observational and empirical data are the same as in Fig. 4.

that the linear terms in δ are absent due to the quadratic dependence of the binding energy per baryon on it. Assuming that higher-order terms in δ_s are negligible, we choose f_s 's similar to f_0 given in Eq. (23). We will parametrize f_s that is independent of δ , so that we keep the nonstrange sector intact. For detailed analysis, we refer to Ref. [72].

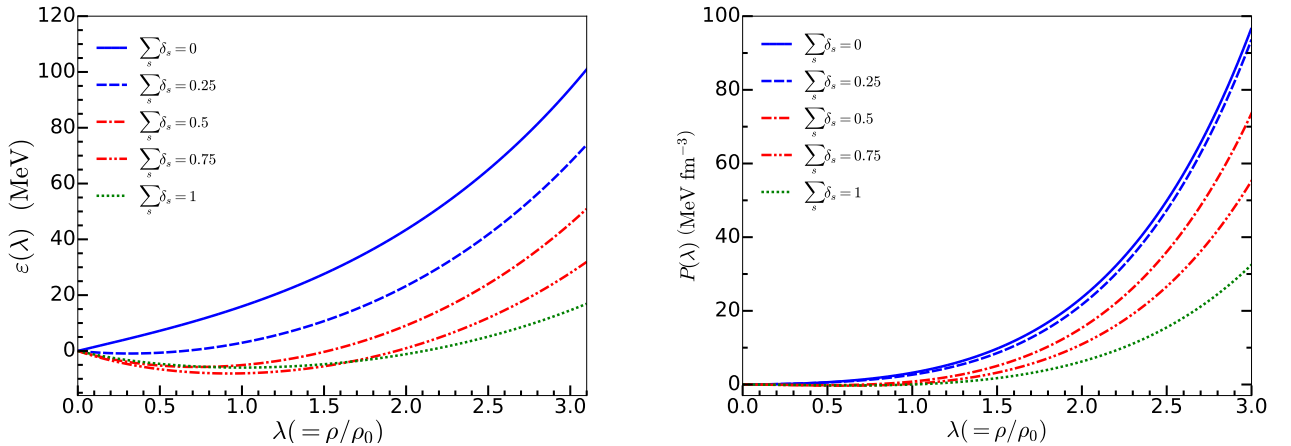


Figure 6. The energy and pressure for baryonic matter as functions of λ . The sum of the parameters δ_s varies from 0 to 1.

In Fig. 6, we draw the results for the energy and pressure as functions of λ with the sum of the parameters δ_s changed from 0 to 1. While $\sum \delta_s = 0$ corresponds to pure neutron matter, $\sum \delta_s = 1$ indicates pure strange matter. The left panel of Fig. 6 shows that as the number of the strange quarks increases, the energy per nucleon starts to decrease. When λ reaches about 0.16, $\varepsilon(\lambda)$ becomes negative and turns positive, which exhibits a behavior similar

Table II. central densities and radii of the neutron stars with two different values of the mass. We take three different values of the incompressibility of nuclear matter with the two different sets of symmetry energy and slope parameters at saturation density ρ_0 . n denotes the central density of neutron matter, λ stands for the corresponding dimensionless central density, and R designates the radius of the neutron star. Note that n_0 corresponds to $\rho_0 = 2.677 \times 10^{14}$ g/cm³.

$K_0, a_{\text{sym}}, L_{\text{sym}}$ [MeV]	$1.4M_\odot$			$2.0M_\odot$		
	n [fm ⁻³]	λ [dimensionless]	R [km]	n [fm ⁻³]	λ [dimensionless]	R [km]
210 MeV, 30 MeV, 50 MeV	0.502	3.136	11.514	0.672	4.198	11.308
240 MeV, 30 MeV, 50 MeV	0.429	2.681	12.121	0.549	3.430	12.094
270 MeV, 30 MeV, 50 MeV	0.385	2.406	12.542	0.477	2.983	12.642
210 MeV, 32 MeV, 50 MeV	0.485	3.030	11.490	0.646	4.036	11.281
240 MeV, 32 MeV, 50 MeV	0.454	2.839	12.110	0.587	3.666	12.074
270 MeV, 32 MeV, 50 MeV	0.434	2.712	12.547	0.550	3.435	12.629
210 MeV, 30 MeV, 60 MeV	0.480	2.997	11.858	0.658	4.115	11.513
240 MeV, 30 MeV, 60 MeV	0.413	2.584	12.435	0.538	3.363	12.299
270 MeV, 30 MeV, 60 MeV	0.372	2.328	12.818	0.468	2.927	12.834
210 MeV, 32 MeV, 60 MeV	0.485	3.032	11.826	0.663	4.146	11.473
240 MeV, 32 MeV, 60 MeV	0.417	2.609	12.426	0.541	3.384	12.272
270 MeV, 32 MeV, 60 MeV	0.375	2.347	12.831	0.470	2.944	12.820

to normal nuclear matter. As the content of the strangeness increases, the saturation point gets lower till it reaches -5.97 MeV at $\lambda \simeq 1$ for pure strange matter. However, strangeness-mixed matter has a shallow saturation point in comparison with nuclear matter [72]. Consequently, the pressure of strangeness-mixed matter becomes weaker as the content of the strangeness increases, as demonstrated in the right panel of Fig. 6. Interestingly, the pressure is lessened by about four times for pure strange matter. This implies that the EoS for strangeness-mixed matter is softer than neutron matter, as discussed in Refs. [100–102].

In Fig. 7, we draw the results for the masses of the strangeness-mixed stars as functions of λ . The short dashed curve depicts the results for the neutron star mass with the parameters $a_{\text{sym}} = 32$ MeV, $L_{\text{sym}} = 60$ MeV, and $K_0 = 240$ MeV used. If we add the strange quarks by 25 %, the mass is not much changed except for the lower density region ($\lambda \geq 3$), as shown by the dashed curve. If we increase the strange quark content, the masses of the strangeness-mixed star become smaller at the same central density. To get the masses of the known neutron stars with higher strangeness content, the central densities should become larger. It implies that as the EoS gets softer, the central density becomes larger. Similar conclusions are found in Refs. [100–105].

The numerical results for the mass-radius relations of the strangeness-mixed stars are depicted in Fig. 8. We fix the parameters for strangeness-mixed matter as $K_0 = 240$ MeV, $a_{\text{sym}} = 32$ MeV, and $L_{\text{sym}} = 60$ MeV, which are considered as our final set of the parameters. We compare the current results with the observed data for the neutron stars. The solid curve designates the result for the neutron stars. When we add the hyperons or the strange quarks to neutron matter, the EoS gets softer, as discussed previously. Consequently, the mass-radius relations become very different from those of the neutron stars. The most prominent feature is that the central density starts to increase, as the strangeness content increases. Assuming that the recently found neutron stars PSR J0740+6620, PSR J0348+0432, and PSR J1614+2330 [12–14] to be strangeness-mixed stars, the corresponding central densities become larger as the strangeness content increases. It also indicates that the strangeness-mixed stars become more compact than the neutron stars, which is understandable. In particular, when the central density gets lower, the mass-radius relations of the strangeness-mixed stars exhibit the propensity to be more shifted to the left. In Table III, varying the strangeness content from 0 to 0.25, we list the corresponding results for the central densities and radii of the strangeness-mixed stars with two different masses $M = 1.4M_\odot$ and $M = 2.0M_\odot$ fixed.

V. SUMMARY AND OUTLOOK

We have investigated the properties of the neutron stars and strangeness-mixed stars, using the equation of the state for both neutron matter and strangeness-mixed matter, which were derived from the medium-modified pion mean-field approach (chiral quark-soliton model) [72]. All the relevant parameters were already fixed in Ref. [72]. A great virtue of this approach is that the medium modifications of the nucleon and hyperons have been considered, in addition to describing the bulk properties of nuclear media. The results for the mass-radius relations were well described in

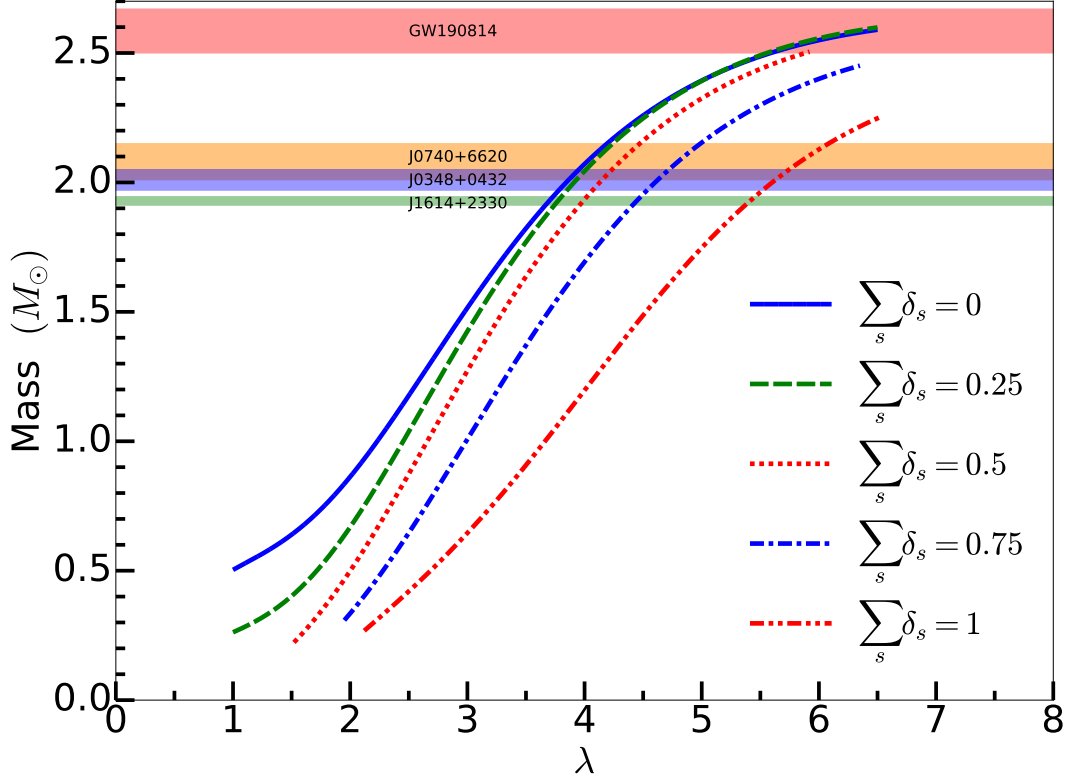


Figure 7. Masses of the strangeness-mixed stars in unit of the solar mass as functions of λ with the strangeness content varied from zero to 1. The values of the symmetry energy, the slope parameter, and the incompressibility at the saturation density are taken as $a_{\text{sym}} = 32 \text{ MeV}$, $L_{\text{sym}} = 60 \text{ MeV}$, and $K_0 = 240 \text{ MeV}$. The observational and empirical data are the same as in Fig. 4.

Table III. The central densities and radii of the strangeness-mixed stars with two different masses, $M = 1.4M_\odot$ and $M = 2.0M_\odot$, fixed. n denotes the central number density, λ is the corresponding ratio n/n_0 , and R stands for the radius of the strangeness-mixed star. We vary the strangeness content δ_s from 0 to 0.25.

δ_s	$1.4M_\odot$			$2.0M_\odot$		
	n [fm $^{-3}$]	λ [dimensionless]	R [km]	n [fm $^{-3}$]	λ [dimensionless]	R [km]
$\delta_s = 0$	0.417	2.609	12.426	0.541	3.384	12.272
$\delta_s = 0.05$	0.423	2.641	12.239	0.544	3.402	12.173
$\delta_s = 0.10$	0.428	2.672	12.064	0.548	3.424	12.075
$\delta_s = 0.15$	0.433	2.706	11.896	0.552	3.450	11.977
$\delta_s = 0.20$	0.439	2.743	11.736	0.557	3.480	11.879
$\delta_s = 0.25$	0.445	2.782	11.580	0.562	3.514	11.780

the current work. The central densities in PSR J0740+6620, PSR J0348+0432, and PSR J1614+2330 [12–14] were obtained to be around $3.5\rho_0$, while the central density corresponding to the neutron star from GW190814 [87] was estimated to be $6.5\rho_0$. We also examined the dependence of the mass-radius relations on the incompressibility K_0 . As K_0 increases, central density becomes lower and the radius increases. To investigate the strangeness-mixed stars, we first examined the equation of state for strangeness-mixed matter, as the strangeness content varied from 0 to 1, which correspond to neutron matter and pure strange matter, respectively. At $\lambda \approx 0.16$, the binding energy becomes negative and turns positive, which behaves as normal nuclear matter. As the content of the strangeness increases,

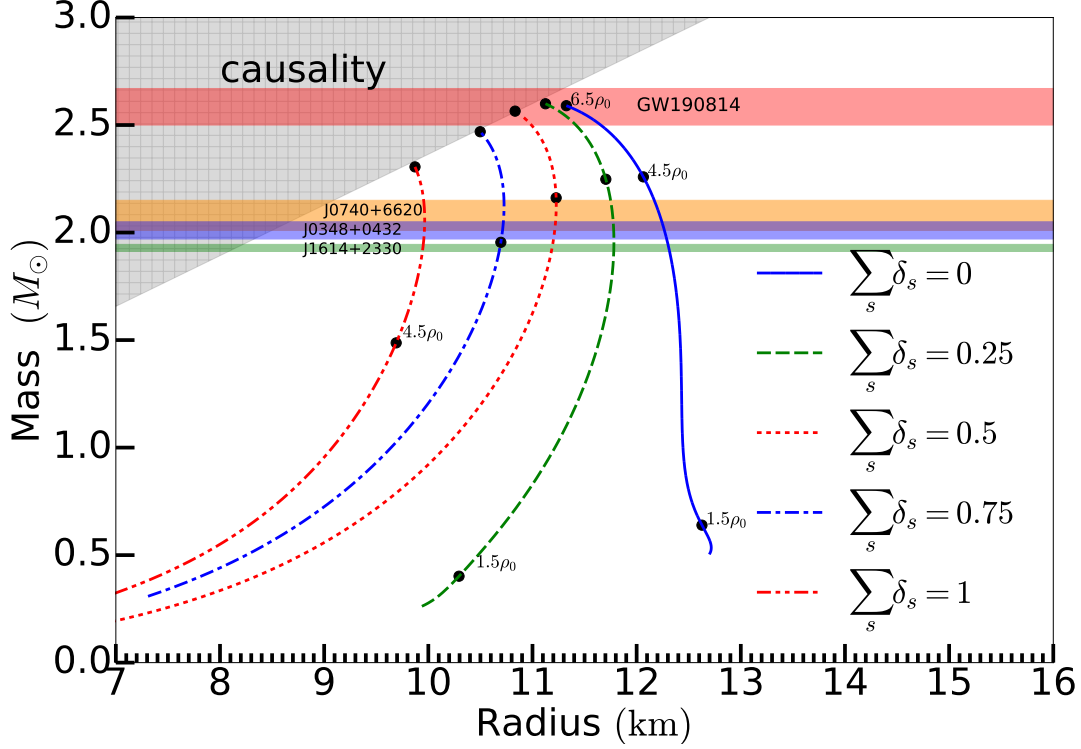


Figure 8. The mass-radius relation of a hyperon-mixed star that has the different portion of hyperons. The parameters of EOS are fixed at values $K_0 = 240$ MeV, $a_{\text{sym}} = 32$ MeV and $L_{\text{sym}} = 60$ MeV. The portion of protons is equal to zero. The results from the experiment and analyses are given in Fig. 4.

the binding energy becomes further lower, though strange matter has a shallow saturation point in comparison with nuclear matter. As a result, the pressure of strange-mixed matter becomes lessened as the strangeness content increases. Note that the pressure is increased by about four times for pure strange matter. This implies that the EoS for strangeness-mixed matter is softened. Thus, the masses of the strangeness-mixed star become smaller at the same central density. We conclude that the strange stars are more compact than the neutron stars.

ACKNOWLEDGMENTS

The present work was supported by Basic Science Research Program through the National Research Foundation (NRF) of Korea funded by the Korean government (Ministry of Education, Science and Technology, MEST), Grant Numbers: 2023R1A2C1008137 (Gh.-S. Y.), 2021R1A2C2093368 (H.-Ch.K.), 2018R1A5A1025563 (H.-Ch.K.), and 2020R1F1A1067876 (U. Y.).

-
- [1] J. M. Lattimer, *Ann. Rev. Nucl. Part. Sci.* **62**, 485 (2012), arXiv:1305.3510 [nucl-th].
 - [2] M. Oertel, M. Hempel, T. Klähn, and S. Typel, *Rev. Mod. Phys.* **89**, 015007 (2017), arXiv:1610.03361 [astro-ph.HE].
 - [3] J. van Paradijs, *Astrophys. J.* **234**, 609 (1979).
 - [4] W. H. G. Lewin, J. van Paradijs, and R. E. Taam, *Space Sci. Rev.* **62**, 223 (1993).
 - [5] R. E. Rutledge, L. Bildsten, E. F. Brown, G. G. Pavlov, and V. E. Zavlin, *Astrophys. J.* **514**, 945 (1999), arXiv:astro-ph/9810288.
 - [6] G. B. Rybicki, C. O. Heinke, R. Narayan, and J. E. Grindlay, *Astrophys. J.* **644**, 1090 (2006), arXiv:astro-ph/0506563.
 - [7] N. A. Webb and D. Barret, *Astrophys. J.* **671**, 727 (2007), arXiv:0708.3816 [astro-ph].
 - [8] A. W. Steiner, J. M. Lattimer, and E. F. Brown, *Eur. Phys. J. A* **52**, 18 (2016), arXiv:1510.07515 [astro-ph.HE].

- [9] D. Alvarez-Castillo, A. Ayriyan, S. Benic, D. Blaschke, H. Grigorian, and S. Typel, *Eur. Phys. J. A* **52**, 69 (2016), arXiv:1603.03457 [nucl-th].
- [10] F. Özel and P. Freire, *Ann. Rev. Astron. Astrophys.* **54**, 401 (2016), arXiv:1603.02698 [astro-ph.HE].
- [11] P. Demorest, T. Pennucci, S. Ransom, M. Roberts, and J. Hessels, *Nature* **467**, 1081 (2010), arXiv:1010.5788 [astro-ph.HE].
- [12] J. Antoniadis *et al.*, *Science* **340**, 6131 (2013), arXiv:1304.6875 [astro-ph.HE].
- [13] E. Fonseca *et al.*, *Astrophys. J.* **832**, 167 (2016), arXiv:1603.00545 [astro-ph.HE].
- [14] E. Fonseca *et al.*, *Astrophys. J. Lett.* **915**, L12 (2021), arXiv:2104.00880 [astro-ph.HE].
- [15] B. P. Abbott *et al.* (LIGO Scientific, Virgo), *Phys. Rev. Lett.* **116**, 131103 (2016), arXiv:1602.03838 [gr-qc].
- [16] B. P. Abbott *et al.* (LIGO Scientific, Virgo), *Phys. Rev. Lett.* **116**, 241103 (2016), arXiv:1606.04855 [gr-qc].
- [17] B. P. Abbott *et al.* (LIGO Scientific, Virgo), *Phys. Rev. X* **9**, 011001 (2019), arXiv:1805.11579 [gr-qc].
- [18] M. Punturo *et al.*, *Class. Quant. Grav.* **27**, 194002 (2010).
- [19] M. Maggiore *et al.*, *Journal of Cosmology and Astroparticle Physics* **03**, 050, arXiv:1912.02622 [astro-ph.CO].
- [20] F. Iacovelli, M. Mancarella, C. Mondal, A. Puecher, T. Dietrich, F. Gulminelli, M. Maggiore, and M. Oertel, *Phys. Rev. D* **108**, 122006 (2023), arXiv:2308.12378 [gr-qc].
- [21] D. Reitze *et al.*, *Bull. Am. Astron. Soc.* **51**, 035 (2019), arXiv:1907.04833 [astro-ph.IM].
- [22] M. Evans *et al.*, (2021), arXiv:2109.09882 [astro-ph.IM].
- [23] M. C. Miller *et al.*, *Astrophys. J. Lett.* **887**, L24 (2019), arXiv:1912.05705 [astro-ph.HE].
- [24] T. E. Riley *et al.*, *Astrophys. J. Lett.* **887**, L21 (2019), arXiv:1912.05702 [astro-ph.HE].
- [25] M. C. Miller *et al.*, *Astrophys. J. Lett.* **918**, L28 (2021), arXiv:2105.06979 [astro-ph.HE].
- [26] T. E. Riley *et al.*, *Astrophys. J. Lett.* **918**, L27 (2021), arXiv:2105.06980 [astro-ph.HE].
- [27] J. M. Lattimer and M. Prakash, *Phys. Rept.* **621**, 127 (2016), arXiv:1512.07820 [astro-ph.SR].
- [28] G. Baym, T. Hatsuda, T. Kojo, P. D. Powell, Y. Song, and T. Takatsuka, *Rept. Prog. Phys.* **81**, 056902 (2018), arXiv:1707.04966 [astro-ph.HE].
- [29] R. W. Romani, D. Kandel, A. V. Filippenko, T. G. Brink, and W. Zheng, *Astrophys. J. Lett.* **934**, L17 (2022), arXiv:2207.05124 [astro-ph.HE].
- [30] D. Diakonov, V. Y. Petrov, and P. V. Pobylytsa, *Nucl. Phys. B* **306**, 809 (1988).
- [31] C. V. Christov, A. Blotz, H.-C. Kim, P. Pobylytsa, T. Watabe, T. Meissner, E. Ruiz Arriola, and K. Goeke, *Prog. Part. Nucl. Phys.* **37**, 91 (1996), arXiv:hep-ph/9604441.
- [32] D. Diakonov, in *Advanced Summer School on Nonperturbative Quantum Field Physics* (1997) pp. 1–55, arXiv:hep-ph/9802298.
- [33] E. Witten, *Nucl. Phys. B* **160**, 57 (1979).
- [34] A. Blotz, D. Diakonov, K. Goeke, N. W. Park, V. Petrov, and P. V. Pobylytsa, *Nucl. Phys. A* **555**, 765 (1993).
- [35] G.-S. Yang, H.-C. Kim, and M. V. Polyakov, *Phys. Lett. B* **695**, 214 (2011), arXiv:1009.5250 [hep-ph].
- [36] G.-S. Yang and H.-C. Kim, *Prog. Theor. Phys.* **128**, 397 (2012), arXiv:1010.3792 [hep-ph].
- [37] H.-C. Kim, M. V. Polyakov, and K. Goeke, *Phys. Rev. D* **53**, 4715 (1996), arXiv:hep-ph/9509283.
- [38] H.-C. Kim, M. V. Polyakov, and K. Goeke, *Phys. Lett. B* **387**, 577 (1996), arXiv:hep-ph/9604442.
- [39] H.-C. Kim, M. Praszalowicz, and K. Goeke, *Phys. Rev. D* **57**, 2859 (1998), arXiv:hep-ph/9706531.
- [40] H.-C. Kim, M. Praszalowicz, and K. Goeke, *Phys. Rev. D* **61**, 114006 (2000), arXiv:hep-ph/9910282.
- [41] T. Ledwig, A. Silva, and H.-C. Kim, *Phys. Rev. D* **82**, 034022 (2010), arXiv:1004.3612 [hep-ph].
- [42] G.-S. Yang and H.-C. Kim, *Phys. Rev. C* **92**, 035206 (2015), arXiv:1504.04453 [hep-ph].
- [43] G.-S. Yang and H.-C. Kim, *Phys. Lett. B* **785**, 434 (2018), arXiv:1807.09090 [hep-ph].
- [44] H.-C. Kim, A. Blotz, M. V. Polyakov, and K. Goeke, *Phys. Rev. D* **53**, 4013 (1996), arXiv:hep-ph/9504363.
- [45] A. Silva, H.-C. Kim, and K. Goeke, *Phys. Rev. D* **65**, 014016 (2002), [Erratum: *Phys.Rev.D* **66**, 039902 (2002)], arXiv:hep-ph/0107185.
- [46] A. Silva, H.-C. Kim, D. Urbano, and K. Goeke, *Phys. Rev. D* **72**, 094011 (2005), arXiv:hep-ph/0509281.
- [47] J.-Y. Kim and H.-C. Kim, *Eur. Phys. J. C* **79**, 570 (2019), arXiv:1905.04017 [hep-ph].
- [48] H.-Y. Won, J.-Y. Kim, and H.-C. Kim, *Phys. Rev. D* **106**, 114009 (2022), arXiv:2210.03320 [hep-ph].
- [49] D. Diakonov, V. Petrov, P. Pobylytsa, M. V. Polyakov, and C. Weiss, *Nucl. Phys. B* **480**, 341 (1996), arXiv:hep-ph/9606314.
- [50] D. Diakonov, V. Y. Petrov, P. V. Pobylytsa, M. V. Polyakov, and C. Weiss, *Phys. Rev. D* **56**, 4069 (1997), arXiv:hep-ph/9703420.
- [51] G.-S. Yang, H.-C. Kim, M. V. Polyakov, and M. Praszalowicz, *Phys. Rev. D* **94**, 071502 (2016), arXiv:1607.07089 [hep-ph].
- [52] H.-C. Kim, M. V. Polyakov, M. Praszalowicz, and G.-S. Yang, *Phys. Rev. D* **96**, 094021 (2017), [Erratum: *Phys.Rev.D* **97**, 039901 (2018)], arXiv:1709.04927 [hep-ph].
- [53] G.-S. Yang and H.-C. Kim, *Phys. Lett. B* **781**, 601 (2018), arXiv:1802.05416 [hep-ph].
- [54] J.-Y. Kim, H.-C. Kim, and G.-S. Yang, *Phys. Rev. D* **98**, 054004 (2018), arXiv:1801.09405 [hep-ph].
- [55] J.-Y. Kim and H.-C. Kim, *Phys. Rev. D* **97**, 114009 (2018), arXiv:1803.04069 [hep-ph].
- [56] G.-S. Yang and H.-C. Kim, *Phys. Lett. B* **801**, 135142 (2020), arXiv:1909.03156 [hep-ph].
- [57] J.-Y. Kim and H.-C. Kim, *PTEP* **2021**, 063D03 (2021), arXiv:1912.01437 [hep-ph].
- [58] J.-Y. Kim, H.-C. Kim, M. V. Polyakov, and H.-D. Son, *Phys. Rev. D* **103**, 014015 (2021), arXiv:2008.06652 [hep-ph].
- [59] J.-M. Suh and H.-C. Kim, *Phys. Rev. D* **106**, 094028 (2022), arXiv:2204.13982 [hep-ph].
- [60] J.-M. Suh, J.-Y. Kim, G.-S. Yang, and H.-C. Kim, *Phys. Rev. D* **106**, 054032 (2022), arXiv:2208.04447 [hep-ph].
- [61] H.-C. Kim, *J. Korean Phys. Soc.* **73**, 165 (2018), arXiv:1804.04393 [hep-ph].
- [62] G. W. Carter and D. Diakonov, *Phys. Rev. D* **60**, 016004 (1999), arXiv:hep-ph/9812445.

- [63] J. Berger and C. V. Christov, Nucl. Phys. A **609**, 537 (1996), arXiv:hep-ph/9607219.
- [64] A. Rakhimov, M. M. Musakhanov, F. C. Khanna, and U. T. Yakhshiev, Phys. Rev. C **58**, 1738 (1998), arXiv:nucl-th/9609049.
- [65] U.-G. Meissner, A. M. Rakhimov, A. Wirzba, and U. T. Yakhshiev, Eur. Phys. J. A **31**, 357 (2007), arXiv:nucl-th/0611066.
- [66] U.-G. Meissner, A. M. Rakhimov, A. Wirzba, and U. T. Yakhshiev, Eur. Phys. J. A **32**, 299 (2007), arXiv:0705.1603 [nucl-th].
- [67] U. Yakhshiev and H.-C. Kim, Phys. Rev. C **83**, 038203 (2011), arXiv:1009.2909 [hep-ph].
- [68] H.-C. Kim, P. Schweitzer, and U. Yakhshiev, Phys. Lett. B **718**, 625 (2012), arXiv:1205.5228 [hep-ph].
- [69] U. Yakhshiev, Phys. Lett. B **749**, 507 (2015), arXiv:1506.06481 [nucl-th].
- [70] E. Witten, Nucl. Phys. B **223**, 422 (1983).
- [71] E. Witten, Nucl. Phys. B **223**, 433 (1983).
- [72] N.-Y. Ghim, G.-S. Yang, H.-C. Kim, and U. Yakhshiev, Phys. Rev. C **103**, 064306 (2021), arXiv:2102.05292 [nucl-th].
- [73] N.-Y. Ghim, H.-C. Kim, U. Yakhshiev, and G.-S. Yang, Phys. Rev. D **107**, 014024 (2023), arXiv:2211.04277 [hep-ph].
- [74] D. Diakonov and V. Y. Petrov, Nucl. Phys. B **272**, 457 (1986).
- [75] D. Diakonov, Prog. Part. Nucl. Phys. **51**, 173 (2003), arXiv:hep-ph/0212026.
- [76] H.-A. Choi and H.-C. Kim, Phys. Rev. D **69**, 054004 (2004), arXiv:hep-ph/0308171.
- [77] G. S. Adkins and C. R. Nappi, Nucl. Phys. B **249**, 507 (1985).
- [78] M. B. Tsang *et al.*, Phys. Rev. Lett. **92**, 062701 (2004).
- [79] T. X. Liu *et al.*, Phys. Rev. C **76**, 034603 (2007), arXiv:nucl-ex/0610013.
- [80] M. A. Famiano, T. Liu, W. G. Lynch, A. M. Rogers, M. B. Tsang, M. S. Wallace, R. J. Charity, S. Komarov, D. G. Sarantites, and L. G. Sobotka, Phys. Rev. Lett. **97**, 052701 (2006), arXiv:nucl-ex/0607016.
- [81] M. B. Tsang, Y. Zhang, P. Danielewicz, M. Famiano, Z. Li, W. G. Lynch, and A. W. Steiner, Phys. Rev. Lett. **102**, 122701 (2009), arXiv:0811.3107 [nucl-ex].
- [82] A. Akmal, V. R. Pandharipande, and D. G. Ravenhall, Phys. Rev. C **58**, 1804 (1998), arXiv:nucl-th/9804027.
- [83] P. Danielewicz and J. Lee, Nucl. Phys. A **922**, 1 (2014), arXiv:1307.4130 [nucl-th].
- [84] N. Hornick, L. Tolos, A. Zacchi, J.-E. Christian, and J. Schaffner-Bielich, Phys. Rev. C **98**, 065804 (2018), [Erratum: Phys.Rev.C 103, 039902 (2021)], arXiv:1808.06808 [astro-ph.HE].
- [85] S. Wang, H. Tong, Q. Zhao, C. Wang, P. Ring, and J. Meng, Phys. Rev. C **106**, L021305 (2022), arXiv:2203.05397 [nucl-th].
- [86] R. Machleidt and F. Sammarruca, Prog. Part. Nucl. Phys. **137**, 104117 (2024), arXiv:2402.14032 [nucl-th].
- [87] R. Abbott *et al.* (LIGO Scientific, Virgo), Astrophys. J. Lett. **896**, L44 (2020), arXiv:2006.12611 [astro-ph.HE].
- [88] L. Brandes, W. Weise, and N. Kaiser, Phys. Rev. D **108**, 094014 (2023), arXiv:2306.06218 [nucl-th].
- [89] V. Vijayan, N. Rahman, A. Bauswein, G. Martínez-Pinedo, and I. L. Arbina, Phys. Rev. D **108**, 023020 (2023), arXiv:2302.12055 [astro-ph.HE].
- [90] B. P. Abbott *et al.* (LIGO Scientific, Virgo), Phys. Rev. Lett. **121**, 161101 (2018), arXiv:1805.11581 [gr-qc].
- [91] M. M. Sharma, W. T. A. Borghols, S. Brandenburg, S. Crona, A. van der Woude, and M. N. Harakeh, Phys. Rev. C **38**, 2562 (1988).
- [92] S. Shlomo and D. H. Youngblood, Phys. Rev. C **47**, 529 (1993).
- [93] Z. Ma, N. Van Giai, H. Toki, and M. L’Huillier, Phys. Rev. C **55**, 2385 (1997).
- [94] D. Vretenar, T. Niksic, and P. Ring, Phys. Rev. C **68**, 024310 (2003), arXiv:nucl-th/0302070.
- [95] B. Ter Haar and R. Malfliet, Phys. Rept. **149**, 207 (1987).
- [96] R. Brockmann and R. Machleidt, Phys. Rev. C **42**, 1965 (1990).
- [97] J. Piekarewicz, Phys. Rev. C **69**, 041301 (2004), arXiv:nucl-th/0312020.
- [98] J. R. Stone, N. J. Stone, and S. A. Moszkowski, Phys. Rev. C **89**, 044316 (2014), arXiv:1404.0744 [nucl-th].
- [99] S. Shlomo, V. M. Kolomietz, and G. Colò, Eur. Phys. J. A **30**, 23 (2006).
- [100] M. Baldo, G. F. Burgio, and H. J. Schulze, Phys. Rev. C **61**, 055801 (2000), arXiv:nucl-th/9912066.
- [101] I. Vidana, A. Polls, A. Ramos, L. Engvik, and M. Hjorth-Jensen, Phys. Rev. C **62**, 035801 (2000), arXiv:nucl-th/0004031.
- [102] S. Nishizaki, T. Takatsuka, and Y. Yamamoto, Prog. Theor. Phys. **105**, 607 (2001).
- [103] S. Nishizaki, T. Takatsuka, and Y. Yamamoto, Prog. Theor. Phys. **108**, 703 (2002).
- [104] H. Chen, M. Baldo, G. F. Burgio, and H. J. Schulze, Phys. Rev. D **84**, 105023 (2011), arXiv:1107.2497 [nucl-th].
- [105] K. Masuda, T. Hatsuda, and T. Takatsuka, Astrophys. J. **764**, 12 (2013), arXiv:1205.3621 [nucl-th].